Proceedings of the
44th IEEE Conference on Decision and Control, and
the European Control Conference 2005
Seville, Spain, December 12-15, 2005

Path Following of Optimal Trajectories Using Preview Control

Asif Farooq
MBDA UK Ltd
Seeker Division
Stevenage SG1 2DA
United Kingdom
Email: asif.farooq@mbda.co.uk

David. J. N. Limebeer
Department of Electrical and Electronic Engineering
Imperial College
London SW7 2BT
United Kingdom
Email: d.limebeer@imperial.ac.uk

Abstract— **This paper investigates the use of optimal preview control for tracking trajectories for air-to-surface missiles. A trajectory is generated off-line by solving a trajectory optimization problem, which incorporates the mission constraints and a model of the missile dynamics. A controller is then designed using optimal preview control to track the reference trajectory on-line and preserve the mission constraints. The control design process involves linearizing and discretizing the missile model and designing an outer guidance loop. By exploiting the structure of the problem, the preview gain sequence can be easily computed via the closed-loop transition matrix and the preview length can be tuned in accordance with the tracking requirements. The preview controller is used up to the radar acquisition range when a seeker is used to detect the target and a closed-loop guidance law is activated. A closed-loop guidance trajectory is presented using this approach and the results are discussed.**

I. Introduction

Current air-to-surface missiles require a low-altitude, stealthy approach to the target followed by a climb and dive (known as a "bunt" maneuver) onto the target at a prescribed impact angle. The problem can be posed as a trajectory optimization problem. Trajectory optimization problems can be solved by either direct or indirect methods. Indirect methods invoke the necessary conditions of optimality (the minimum principle) to obtain solutions. Alternatively, numerical solutions can be obtained via discretization and nonlinear programming (known as direct methods). The solution of a trajectory optimization problem generates a vector of open-loop controls and optimal state trajectories.

Following the trajectory optimization stage it is necessary to design a feedback controller to track the reference trajectory on-line. The feedback controller is used to counteract such things as disturbances (e.g. gusts) and modeling errors. In this paper the use of preview control is examined to track bunt trajectories. In preview control the use of future information (in this case a segment of the desired trajectory profile) is incorporated into the controller design to improve the tracking accuracy. This is combined with linear quadratic regulation to null deviations from the equilibrium condition, effectively resulting in a two degree-of-freedom controller. The preview controller is used up until the acquisition range when a seeker is used to acquire the target. A closed-loop guidance law is then used to satisfy the terminal accuracy and impact angle constraints. The methodology for designing the preview controller is detailed and the tracking of an example off-line optimal trajectory is presented.

Previous Work

Preview control for state-space models was first proposed in [1] for discrete-time tracking of a reference trajectory over a fixed horizon. Early examples for a vehicle suspension problem are considered in [2]–[4]. These examples are disturbance rejection problems, though it can be shown that the tracking problem is a special case of the disturbance rejection problem. The reader is also referred to [5] for an overview of preview control in the general context of digital tracking control. Another area of application for which preview control has been popular is terrain following. Examples of terrain following for helicopters [6] and missiles [7] have been studied. Automated road tracking using preview control is studied in [8]. Recent work has focused on H_∞ versions of preview control. The linear discrete time H_∞ solution for output tracking with preview is presented in [9]. In [10] the preview problem is cast in a unified framework where the continuous and discrete time H_2 and H_∞ solutions are derived using the calculus of variations. An example of a vehicle durability simulator is then presented.

Terminal bunt trajectories were first considered in [11] using linear quadratic control. A theoretical analysis of the bunt maneuver is considered in [12]; a direct method is used to compute an optimal bunt trajectory and the indirect method (based on the minimum principle) is invoked to examine the structure of the solution for a relatively simple problem. The indirect method is valuable for providing insights into the nature of solutions and yields high-accuracy solutions. This level of pre-analysis is more difficult for more complex models and problems, and most practical trajectory optimization involve the use of direct methods. Examples of three-dimensional bunt trajectories calculated using direct methods are presented in [13] for skid-to-turn steering and [14] for bank-to-turn steering. These latter two papers also consider the imposition of radar imaging constraints into the trajectory optimization problem.

II. Missile Model

The open-loop missile dynamics can be described by the following set of equations that apply in the vertical plane.

0-7803-9568-9/05/$20.00 ©2005 IEEE

Flight-path axes are used for the translational equations and body-fixed axes for the rotational motion:

$$\dot{V}_t = \left(\frac{T}{m}\right)cos(\alpha) - \frac{Q_d S_r C_{xw}}{m} - g\ sin(\gamma) \quad (1)$$

$$\dot{\alpha} = \frac{Q_d S_r C_{zw}}{mV_t} + \left(\frac{g}{V_t}\right)cos(\gamma) + q - \left(\frac{T}{mV_t}\right)sin(\alpha) \quad (2)$$

$$\dot{\theta} = q \quad (3)$$

$$\dot{q} = \frac{Q_d S_r l C_m}{I_{yy}} \quad (4)$$

$$\dot{R}_{sx} = (V_t)cos(\gamma) \quad (5)$$

$$\dot{R}_{sz} = -(V_t)sin(\gamma). \quad (6)$$

The state variables are the speed V_t, the angle of incidence α, the pitch angle θ, the pitch rate q, downrange R_{sx} and altitude R_{sz}. The airframe parameters are the mass m, the pitch moment of inertia I_{yy}, the reference area S_r and the reference length l, and g is the acceleration due to gravity. The coefficients C_{xw} and C_{zw} are the aerodynamic coefficients in flight path axes and $Q_d = \frac{1}{2}\rho V_t^2$ is the dynamic pressure where ρ is the air density. The applied thrust is denoted by T. The flight path angle is related to the pitch angle and angle of incidence by an algebraic relationship ($\gamma = \theta - \alpha$). The missile system is non-minimum phase, which imposes a limitation on the achievable tracking accuracy. The aerodynamic coefficients C_x and C_z are conventionally supplied in body axes and are related to the flight path axes coefficients C_{xw} and C_{zw} using:

$$\begin{bmatrix} C_{xw} \\ C_{zw} \end{bmatrix} = \begin{bmatrix} cos(\alpha) & -sin(\alpha) \\ sin(\alpha) & cos(\alpha) \end{bmatrix} \begin{bmatrix} C_x \\ C_z \end{bmatrix}. \quad (7)$$

The body axes aerodynamic coefficients can be expressed as linear functions at fixed flight conditions using stability derivatives. The aerodynamic coefficients are calculated as:

$$C_x = C_{x0} + kC_{x\alpha}\alpha^2 \quad (8)$$

$$C_z = C_{z0} + C_{z\alpha}\alpha + C_{z\delta}\delta_q \quad (9)$$

$$C_m = C_{m0} + C_{m\alpha}\alpha + \frac{C_{mq}q}{V_t} + C_{m\delta}\delta_q \quad (10)$$

i.e. $C_{z\alpha} = \frac{\partial C_z}{\partial \alpha}$ with the other derivatives being defined in a similar fashion. Fixed stability derivatives are used in this study. The vehicle is controlled using the fin elevator δ_q, which generates a net torque. The torque generates lift by developing an appropriate angle of incidence α.

Although it is possible to design the preview controller using fin angle as the control input, it is more convenient to augment the model equations to implement an acceleration feedback autopilot. The pitch autopilot improves the stability of the airframe and the missile is controlled by specifying a pitch acceleration demand. As the pitch acceleration can be measured via accelerometers this provides a convenient means to design an acceleration feedback autopilot. The acceleration achieved (at the center of gravity) A_{mz} can be computed using the algebraic equation:

$$A_{mz} = \frac{\rho V_t^2 S_r \left(C_{z0} + C_{z\alpha}\alpha + C_{z\delta}\delta_q\right)}{2m}. \quad (11)$$

The autopilot contains integral action and feedback signals (pitch acceleration and pitch body rate). An appropriate choice of feedback gains ensures a fast, well damped response to reference acceleration demands. The autopilot dynamics can be modeled by introducing a new state which corresponds to the integrator output in the autopilot. The fin angle deflection can then be obtained via an additional algebraic equation. To model the autopilot dynamics the vehicle equations need to be augmented by:

$$\dot{x}_p = (A_{zd} - A_{mz})k_1 - k_2(A_{mz} + g\ cos(\theta)) - k_3 q \quad (12)$$

$$\delta_q = x_p - k_4 q. \quad (13)$$

A_{zd} is the demanded acceleration which is the input to the pitch autopilot and $k_1, ..k_4$ are the autopilot gains. With these equations the missile system is completely described. The airframe parameters and autopilot gains are shown in Table I.

TABLE I
AIRFRAME PARAMETERS

Parameter	Units	Value
Mass (m)	kg	1200
Pitch inertia (I_{zz})	kgm^2	1500
Reference area (S_r)	m^2	0.31
Reference length (l)	m	0.63
Axial derivatives ($C_{x0}, C_{x\alpha}$)	rad^{-1}	0.17, 0.68
Lift derivatives ($C_{z0}, C_{z\alpha}, C_{z\delta}$)	rad^{-1}	-0.39,-24.64 -2.64
Pitch derivatives ($C_{m0}, C_{mq}, C_{m\delta}, C_{m\alpha}$)	rad^{-1}	0.04,-66.15 -9.45,-5.73
Drag coefficient (k)	-	5.0
Autopilot gains (k_1, k_2, k_3, k_4)	-	0.96, -0.09 -25.20,-1.71

A. Obtaining a linear discrete time model

It is necessary to manipulate the state-space equations to implement the preview controller. The first simplification is to decouple the speed equation, (1) from the preview controller. The speed is assumed to be controlled independently and the thrust may be regulated to follow a prescribed speed profile using a Mach autopilot. This may be necessary as the speed profile might need to be tightly controlled due to tactical requirements. More subtly, the speed affects the turn radius (and hence the pitch acceleration demand).

The second simplification concerns the downrange equation, which is removed from the state-space equations. This is because it is more convenient for the independent variable in the differential equations to be downrange rather than time. The downrange is a monotonic variable and is a suitable choice of independent variable. The preview controller then

utilizes a look-ahead preview distance in terms of downrange. This is more convenient from an implementation perspective as the look-ahead distance can be adjusted for changes in the missile speed. The time to downrange transformation is simple to accomplish and is implemented by dividing each equation by the downrange rate (5). This simplification reduces the state dimension and the state vector is now $x = [\alpha, \theta, q, R_{sz}, x_p]^T$. An equilibrium flight condition (trimmed flight at fixed altitude with a constant speed of 272 m/s) was chosen and the missile equations were numerically linearized about this condition. The trim condition was found to be $x_{trim} = [0.0188, 0.0188, 0, 60, 0.0]$ which corresponds to straight and level flight at 60 m height with a small (0.0188 rad) angle of incidence. At trim -1 g pitch acceleration is demanded to counteract gravity. The output of the system is chosen to be the height achieved. The linearization procedure results in the following system matrices:

$$\bar{A} = \begin{bmatrix} -1.06 & 0 & 0.81 & 0 & -0.11 \\ 0 & 0 & 1 & 0 & 0 \\ -33.88 & 0 & -96.8 & 0 & -55.9 \\ 272 & -272 & 0 & 0 & 0 \\ 251.5 & -0.017 & 71.35 & 0 & 26.9 \end{bmatrix} \quad (14)$$

$$\bar{B} = \begin{bmatrix} 0 \\ 0 \\ 0 \\ 0 \\ 0.96 \end{bmatrix} \quad (15)$$

$$\bar{C} = \begin{bmatrix} 0 & 0 & 0 & 1 & 0 \end{bmatrix}, \bar{D} = 0. \quad (16)$$

It can easily be verified that the linearized system is both controllable and observable. The time to downrange transformation has the effect of scaling the above system matrices $\bar{A}$ and $\bar{B}$ by the nominal speed (272 m/s). The linearized system matrices $(\bar{A}, \bar{B}, \bar{C}, \bar{D})$ were then discretized using a zero-order hold method with a sample time of 0.01 s. The discrete time system equations are expressed as:

$$x(k+1) = Ax(k) + Bu(k) \quad (17)$$

$$y(k) = Cx(k), \quad (18)$$

where A, B and C are the discrete time system matrices and $D = 0$. It should be noted that the linearized system applies to the perturbation variables from the trim condition and the control $u(k)$ is a sampled perturbation control signal. The perturbation control needs to be added to the trim control to get the actual control. In this paper the model is linearized at one operating point only, which has the advantage of simplifying the controller structure. The design can be adapted to multiple operating points using a gain-scheduling approach.

B. Designing the preview controller

In this study the objective is to track a desired height profile. This requirement is encapsulated by the following infinite horizon cost function:

$$J = \frac{1}{2}\sum_{k=0}^{\infty} e^T(k)Qe(k) + u^T(k)Ru(k), \quad (19)$$

where the reference signal is denoted by $y_d(k)$ and $e(k) = y_d(k) - y(k)$ is the tracking error and Q and R penalize the tracking error and control energy respectively. The discrete time system matrices can be augmented by a command generator system which models the preview part of the system:

$$x_d(k+1) = A_d x_d(k) + B_d w_d(k) \quad (20)$$

$$y_d(k) = C_d x_d(k), \quad (21)$$

where

$$A_d = \begin{bmatrix} 0 & 1 & 0 & \cdots & 0 \\ 0 & 0 & 1 & \cdots & 0 \\ \vdots & \vdots & \vdots & \ddots & \vdots \\ 0 & \cdots & \cdots & \cdots & 1 \\ 0 & \cdots & \cdots & \cdots & 0 \end{bmatrix}, B_d = \begin{bmatrix} 0 \\ 0 \\ 0 \\ \vdots \\ 1 \end{bmatrix} \quad (22)$$

$$C_d = \begin{bmatrix} 1 \\ 0 \\ 0 \\ \vdots \\ 0 \end{bmatrix}^T, x_d(k) = \begin{bmatrix} y_d(k) \\ y_d(k+1) \\ y_d(k+2) \\ \vdots \\ y_d(k+N_p-1) \end{bmatrix}. \quad (23)$$

The state of the command generator $x_d(k)$ is composed of sampled values of the reference signal over the preview horizon (of length N_p). The matrix A_d implements a shift register operation. The input to the command generator system is the reference signal at the end of the preview horizon $y_d(k+N_p)$. Although the example in this paper is for tracking a single signal, the tracking of multi-dimensional signals can easily be accommodated (see [8]).

In order to recast the preview optimal control problem in a standard LQG form, it is convenient to augment the plant and preview system to get:

$$\begin{bmatrix} x(k+1) \\ x_d(k+1) \end{bmatrix} = \begin{bmatrix} A & 0 \\ 0 & A_d \end{bmatrix} \begin{bmatrix} x(k) \\ x_d(k) \end{bmatrix} + \begin{bmatrix} B \\ 0 \end{bmatrix} u(k) + \begin{bmatrix} 0 \\ B_d \end{bmatrix} w_d(k). \quad (24)$$

If we define an augmented vector by stacking $x(k)$ and $x_d(k)$ and define augmented system matrices for the plant and preview systems, i.e:

$$x_a(k) = \begin{bmatrix} x(k) \\ x_d(k) \end{bmatrix}, A_a = \begin{bmatrix} A & 0 \\ 0 & A_d \end{bmatrix}$$

$$B_a = \begin{bmatrix} B \\ 0 \end{bmatrix}, B_{da} = \begin{bmatrix} 0 \\ B_d \end{bmatrix}. \quad (25)$$

The tracking error can now be written as:

$$e(k) = [C - C_d]x_a(k) = C_a x_a(k). \quad (26)$$

With these definitions the cost function can be expressed in terms of the augmented system as:

$$J = \frac{1}{2}\sum_{k=0}^{\infty} x_a(k)^T Q_a x_a(k) + u^T(k)Ru(k). \quad (27)$$

The problem is a discrete linear quadratic regulator problem and standard theory [15] can be invoked to obtain the solution as:

$$u(k) = -Kx_a(k) = [-K_1 - K_2] \begin{bmatrix} x(k) \\ x_d(k) \end{bmatrix} \quad (28)$$

$$K = MB_a{}^T SA_a \quad (29)$$

$$M = \left(B_a{}^T SB_a + R\right)^{-1}, \quad (30)$$

where the steady state Riccati equation is used to obtain S:

$$S = A_a{}^T SA_a + Q_a - A_a{}^T SB_a MB_a^T SA_a. \quad (31)$$

The use of the augmented system induces a partitioning of S. If we partition S as:

$$S = \begin{bmatrix} S_{11} & S_{12} \\ S_{21} & S_{22} \end{bmatrix}, \quad (32)$$

then S_{11} corresponds to the plant-only part of the system and S_{12} corresponds to the preview part of the system; S_{11} is the solution of a plant-only Ricatti equation. The S_{12} partition can be obtained through a simple linear recursive equation. The gain matrices K_1 and K_2 can be easily shown (by expanding (29)) to be:

$$K_1 = \left(B^T S_{11} B + R\right)^{-1} B^T S_{11} A \quad (33)$$

$$K_2 = \left(B^T S_{11} B + R\right)^{-1} B^T S_{12} A_d \quad (34)$$

The gain K_1 is just the standard LQR gain for the plant-only system and is thus independent of the preview system. The gain sequence K_2 multiplies by $y_d(k+i)$ for $i = 0, 1, 2, ...N_p - 1$ since $x_d(k)$ is composed of the reference signal N_p units into the future. To compute K_2 we require the S_{12} partition. This can be achieved by expanding (31) to obtain a recursive relationship for S_{12}. The details are omitted here, but it can easily be shown that the S_{12} partition can be reduced to the following linear relationship:

$$S_{12} = \Phi_c^T S_{12} A_d + Q_{12a}, \quad (35)$$

where Φ_c is the closed-loop transition matrix (which is related to S_{11}) and Q_{12a} is the upper right partition of Q_a. If we denote the i^{th} column of S_{12} by S_{12i} with $i = 1, 2, ...N_p$ then,

$$S_{12}A_d = \begin{bmatrix} 0 \\ S_{121} \\ S_{122} \\ \vdots \\ S_{12N_p-1} \end{bmatrix}^T. \quad (36)$$

The matrix Q_{12a} can be split into columns Q_{12ia}, for $i = 1, 2...N_p$ and simplified:

$$Q_{12a} = \begin{bmatrix} Q_{121a} & Q_{122a} & \dots & Q_{12N_pa} \end{bmatrix} \quad (37)$$

$$= -C^T Q C_d$$

$$= -C^T Q \begin{bmatrix} 1 & 0 & \dots & 0 \end{bmatrix} \quad (38)$$

$$= \begin{bmatrix} -C^T Q & 0 & 0 & \dots & 0 \end{bmatrix}. \quad (39)$$

By substituting (39) and (36) into (35), the partition S_{12} can be neatly expressed as:

$$S_{12i} = -(\Phi_c^T)^{i-1} C^T Q, i = 1, 2, ...N_p. \quad (40)$$

The expression (40) is a recursive solution used to obtain the S_{12} partition. Once the S_{12} partition is computed the preview gain sequence can be calculated through (34). The amount of preview required depends on the closed-loop poles, which are the eigenvalues of Φ_c. For fast closed-loop poles the preview horizon can be reduced. The poles of Φ_c are always inside the unit circle and the preview gain will decay to zero. After three to five closed-loop time constants, there is little benefit in increasing the preview length further.

C. Terminal guidance

The preview controller is used up until the acquisition range when a seeker detects the target (in a relative frame of reference). A seeker is required to obtain high angular accuracy, reducing the miss distance. The acquisition range is dependent on the radiated power, the target characteristics and atmospheric conditions. In this study the acquisition range is assumed fixed at approximately $1.8\,\text{km}$. A terminal guidance law [16] is used in the terminal phase. This guidance law is designed to minimize both miss distance and impact angle error and was found to be effective in simulations. To minimize the terminal incidence a switch to zero pitch acceleration is specified at a finite range-to-go ($120\,\text{m}$) - this tends to increase the impact angle error slightly but satisfactory solutions are obtainable.

An alternative solution method might be to use the finite horizon preview controller [1]. This, however, may be less effective, since it requires the missile position to be calculated in an absolute frame. Due to the build-up of inertial position errors over time and errors introduced by co-ordinate transformations this method is unlikely to achieve the terminal accuracy requirements. Another recommendation against this approach is that nonlinearities are more prevalent near the impact point, since the missile angles can change very rapidly.

A problem arises when the look-ahead distance in downrange exceeds the terminal downrange position (e.g. if the seeker acquisition range is very short), since the preview controller then does not have information beyond the end of the horizon. The problem was resolved by setting the height values beyond the terminal downrange to be equal to the final height sample or the desired final height. The current study also assumes that the state deviation vector can be measured perfectly. This is an unrealistic assumption and more practically the state has to be estimated through noise corrupted sensor measurements.

III. Results

A simple example of tracking an optimal trajectory that was computed off-line is presented. The trajectory is characterized by a period of low-altitude flight (to minimize exposure) followed by a bunt maneuver to obtain a prespecified impact angle. In these problems a suitable cost

function for the open-loop optimization is the time integral of the height squared. This problem can be posed as a trajectory optimization problem and numerical methods can be employed to obtain a solution. An optimal open-loop trajectory for this problem was obtained through a trajectory optimization procedure (the reader is referred to [13] for a detailed description of the methodology).

The optimal trajectory computed numerically is a bunt maneuver with a terminal downrange ordinate of $10\,\text{km}$ and an impact angle of $15\,\text{deg}$ from a vertical reference. An acceleration demand limit of $3\,\text{g}$ was imposed. The optimal solution for this example requires a bang-bang type of control (see [12]). As the open-loop simulations result in saturation of the controls, some control reserve (approximately $1.5\,\text{g}$) is assumed in the closed-loop simulations. Similarly, any path constraints in the open-loop optimization would require some slack as the method only deals with these constraints in a soft manner. Full thrust is assumed in the closed-loop simulations, which is a good approximation to the optimal thrust profile obtained in previous studies (see [12] and [14]).

The actual control signal is obtained by calculating the perturbed control signal (which contains the feedback and feedforward components) and adding this to the trim control ($-1\,\text{g}$). The simulations were implemented on the nonlinear model, which includes actuator dynamics with angle limits of $0.45\,\text{rad}$. Tuning of the preview length N_p and the weighting matrices Q and R were required. A preview length of 600 samples, $Q = 50.0$ and $R = 10.0$ was used in these simulations. This choice of weighting results in closed-loop poles at 0.31, 0.88+/-0.09j and 0.99+/-0.01j, which are all within the unit circle. The preview length of 600 samples corresponds to a look-ahead distance of approximately $1.6\,\text{km}$ in downrange for the nominal speed of $272\,\text{m/s}$. If the missile speed increases the look-ahead distance increases as well.

The state trajectories obtained through trajectory optimization are computed over a variable step integration grid. To implement the preview controller the downrange/height profile needs to be interpolated at every time step. The procedure for doing this is as follows:

1) Calculate the missile current position in downrange and the current height.
2) Interpolate the optimal trajectory to obtain the desired height at the current downrange.
3) Using the current speed, the flight path angle, the sample time ($0.01\,\text{s}$) and the preview length calculate the look-ahead distance in downrange.
4) Interpolate the optimal height/downrange curve at N_p equally spaced points ahead in downrange. This results in a N_p by two dimensioned matrix of downrange, height co-ordinates and produces the trajectory segment which is used in the preview controller.

To test the regulation properties of the controller initial condition errors of $2\,\text{m}$ in altitude and $2\,\text{deg}$ in the angle of incidence were imposed. This corresponds to the realistic case in which the initial missile position may not be on the optimal trajectory (due to disturbances and/or launch errors). The example presented assumes that the missile can compute its position through an inertial navigation system, combined with other sensor information and thus knows its position relative to the desired trajectory. Results are displayed in Figs. 1 and 2 which show the open/closed-loop trajectories, the tracking error and the open-loop/closed-loop controls respectively. The tracking error is computed by calculating the error in height at sampled points along the trajectory. In the plots for the closed-loop control the pitch acceleration demand is displayed as well as the achieved fin angle.

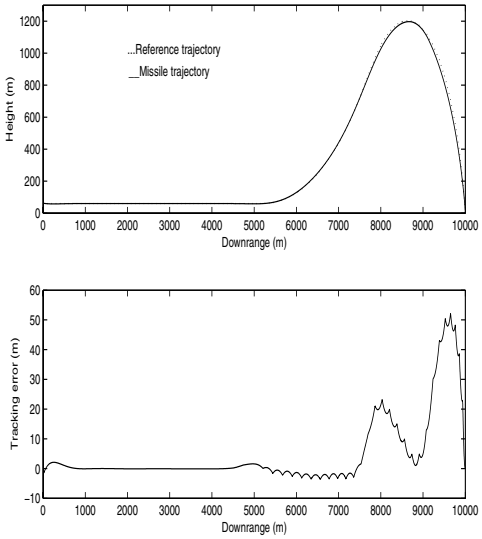

Fig. 1. Trajectories and tracking error for unconstrained bunt

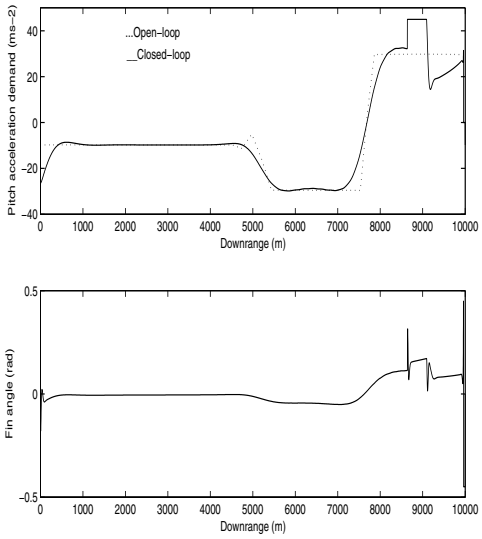

Fig. 2. Control signal for unconstrained bunt

The initial perturbation in the height and angle of incidence are regulated to zero using an initial transient of $-2.5\,\text{g}$ in pitch acceleration. This is evident in the tracking error profile for position, there is a slight overshoot in height due to the angle of incidence perturbation. Following this the tracking error is kept small throughout the terrain following phase. There is a slight increase in tracking error prior to

the bunt at approximately $4.6\,\mathrm{km}$ in downrange. This is because the open-loop trajectory has a sharp corner at the downrange where the climb commences and the preview controller appears to smooth this out by letting the missile dip slightly before converging on the segment of the curve corresponding to the missile climb. The resulting control action is smoothed as a result. The missile climb requires approximately $-3\,\mathrm{g}$ demanded pitch acceleration. After acquisition at approximately $8.5\,\mathrm{km}$ downrange the controller switches to the impact angle guidance law. This enables the missile to satisfy the impact angle and miss distance. The preview controller has the desirable effect of smoothing the bang-bang open-loop control signal.

The performance metrics of interest in this simulation are a miss distance of $1.3\,\mathrm{m}$, an impact angle error of $2.7\,\mathrm{deg}$ and incidence at impact of $4.6\,\mathrm{deg}$. The maximum tracking error is approximately $50\,\mathrm{m}$. This occurs after acquisition and indicates that the closed-loop guidance law results in a different path to the target compared with the open-loop trajectory (though the two trajectories converge as the tracking error reduces to zero at the impact point). During the period when the preview controller is used the maximum tracking error is approximately $20\,\mathrm{m}$. Switching to a closed-loop guidance law and nulling the acceleration demands near the impact point induce transients on the control signal (see Fig. 2).

The effect of reducing the preview length to 400 samples was investigated for this case. A reduction in the preview length leads to higher tracking errors. This can be mitigated by increasing the bandwidth of the system (via a reduction in the control weighting), but a higher bandwidth system was found to lead to increased control action for small initial condition errors. This demonstrates the interaction between the feedback and feedforward parts of the system in preview control. It is noticeable that the tracking error increases during the climb since the linear model is less accurate at larger climb angles and angles of incidence. This aspect of performance might be improved by using a sequence of linear models. Nonetheless the performance in the nonlinear simulation is surprisingly good given the relatively simple linearization procedure.

IV. Conclusions

This paper has investigated the use of preview control in a trajectory following application. The problem requires a missile to track a precomputed optimal trajectory for an air-to-surface terminal guidance problem. The precomputed trajectory is a bunt trajectory with terminal angle constraints and was obtained through an trajectory optimization procedure. The controller used combines preview control for on-line tracking of the optimal trajectory with a closed-loop guidance law to achieve the terminal constraints. This combination appears to be a promising method for closed-loop guidance. Future work will focus on i) enhancing the model and conducting 3D studies; ii) looking at a measurement feedback version of the preview controller using a state estimator; iii) investigating different versions of preview such as H_∞ formulations and looking at comparisons with other path following methods.

Acknowledgements

This work was funded by MBDA UK Ltd.

References

[1] M. Tomizuka and D. E. Whitney, "Optimal Discrete Finite Preview Problems (Why and How is Future Information Important?)," *ASME Journal of Dynamic Systems, Measurement and Control*, pp. 319–325, Dec. 1975.

[2] S. H. Roh and Y. Park, "Stochastic Optimal Preview Control of An Active Vehicle Suspension," *Journal of Sound and Vibration*, vol. 220, no. 2, pp. 313–330, 1999.

[3] A. Hac, "Optimal Linear Preview Control of Active Vehicle Suspensions," in *Proc. IEEE Conference on Decision and Control*, Honolulu, Hawaii, December 1996, pp. 2779–2784.

[4] G. Prokop and R. S. Sharp, "Performance enhancement of limited-bandwidth active automotive suspensions by road preview," *IEE Proceedings on Control Theory and Applications*, vol. 142, no. 2, pp. 140–148, March 1995.

[5] M. Tomizuka, "On the Design of Digital Tracking Controllers," *ASME Journal of Dynamic Systems, Measurement and Control*, vol. 115, pp. 412–418, June 1993.

[6] G. Liborio, N. Paulino, R. Cunha, C. Silvestre, and I. M. Ribeiro, "Terrain following preview controller for model-scale helicopters," in *Proceedings of the 11th International Conference on Advanced Robotics*, Coimbra, Portugal, June-July 2003.

[7] D. Li, D. Zhou, Z. Hu, and H. Hu, "Optimal Preview Control Applied to Terrain Following Flight," in *Proc. IEEE Conference on Decision and Control*, Orlando, Florida, December 2000, pp. 211–216.

[8] R. S. Sharp and V. Valtetsiotis, "Optimal Preview Car Steering Control," *ASME Journal of Vehicle Systems Dynamics (Supplement)*, vol. 35, pp. 101–117, 2001.

[9] A. Cohen and U. Shaked, "Linear Discrete Time H_∞ Optimal Tracking with Preview," in *Proc. IEEE Conference on Decision and Control*, Dec. 1995, pp. 2555–2561.

[10] L. Mianzo and H. Peng, "A Unified Framework for LQ and H_∞ Preview Control Algorithms," in *Proc. IEEE Conference on Decision and Control*, Tampa, Florida, Dec. 1998, pp. 2816–2821.

[11] H. C. E. Kim and Y. Lee, "Terminal Guidance of Missiles Maneuvering in the Vertical Plane," in *Proc. AIAA Guidance, Navigation and Control Conference*, San Diego, California, July 1996.

[12] J. Cleminson, R. Zbikowski, and S. Subchan, "Optimal Bunt Trajectory: An Analysis By The Indirect Method," in *Proc. AIAA Guidance, Navigation and Control Conference*, Austin, Texas, 2003.

[13] A. Farooq and D. J. N. Limebeer, "Trajectory Optimization for Air-to-Surface Missiles with Imaging Radars," *AIAA Journal of Guidance, Control and Dynamics*, vol. 25, no. 5, pp. 876–888, September-October 2002.

[14] ——, "Bank-to-turn Missile Guidance with Radar Imaging Constraints," *AIAA Journal of Guidance, Control and Dynamics*, to appear.

[15] B. D. O. Anderson and J. B. Moore, *Optimal Control: Linear Quadratic Methods*. New Jersey: Prentice-Hall International, 1989.

[16] I. R. Manchester and A. V. Savkin, "Circular Navigation Guidance Law for Precision Missile/Target Engagements," in *Proc. IEEE Conference on Decision and Control*, Las Vegas, Nevada, December 2002, pp. 1287–1292.